scientific reports

Check for updates

OPEN

Analysis of the molecular mechanisms of ulcerative colitis and atherosclerosis by microarray data

Min Wu[1], Dong Liu[2], Xiaoman Xiong[1], Qiang Su[1], Yi Xiang[1], Lang Shen[1], Zhenxiang An[3]✉ & Xiaofang Yang[1]✉

Adults can develop ulcerative colitis (UC), a chronic inflammatory illness of the colon, while atherosclerosis (AA) is a chronic inflammatory disease of the blood vessels caused by a range of risk factors. Prior research has demonstrated that UC increases the risk of AA, although the underlying pathological mechanisms are not entirely understood. The purpose of this work was to discover differentially expressed genes (DEGs) in UC and AA and investigate their molecular processes using a bioinformatics method. The UC (GSE36807) and AA (GSE28829) datasets were obtained from the Gene Expression Omnibus (GEO) database. Following the identification of genes that are differentially expressed in common with UC and AA, functional annotation, the construction of protein-protein interaction (PPI) networks and modules, the identification of hub genes, and co-expression analysis were carried out. A total of 105 (including 92 up-regulated and 13 down-regulated genes) DEGs were selected for correlation analysis in the above two datasets, and after Gene Ontology (GO) and Kyoto Encyclopedia of Genes and Genomes (KEGG) functional analysis immune responses, cytokines, and chemokines were found to play crucial roles in both diseases. Finally, a total of 16 hub genes were identified by CytoHubba and MCODE plugins in Cytoscape, including Chemokine (C-C motif) ligand 4(CCL4), Toll-like receptor 2 (TLR2), Integrin Beta 2(ITGB2), Chemokine (C-C motif) Receptor 1(CCR1), Toll-Like Receptor 8 (TLR8), Fc Fragment of IgG Receptor IIa (FCGR2A), Neutrophil Cytosolic Factor 2(NCF2), Leukocyte immunoglobulin-like receptor B2(LILRB2), FGR proto-oncogene, Src family tyrosine kinase(FGR), Intercellular Adhesion Molecule 1 (ICAM1), Caspase 1(CASP1), Matrix Metallopeptidase 9(MMP9), Cluster of Differentiation 163(CD163), Complement Component 5a Receptor 1 (C5AR1), Neutrophil Cytosolic Factor 4 (NCF4), Selectin P (SELP). This study discovered a link between UC and AA, as well as shared hub genes and pathways, which may bring new insights into the processes of UC and AA.

Keywords Ulcerative colitis, Atherosclerosis, Bioinformatics, DEG's, Hub genes

Atherosclerosis (AA) is a chronic inflammatory disease of the blood vessels characterized by the deposition of various cells, lipids, and tissue debris within the arterial walls[1]. Ulcerative colitis (UC) is a chronic inflammatory disease of the colon, often associated with genetic, environmental, and immune dysregulation factors[2]. UC has a strong association with AA development. Studies dating back to 1996 indicate that UC patients face an increased risk of AA and that the risk of atherosclerotic cardiovascular disease is 2–4 times higher in UC patients compared to non-UC individuals[3,4]. AA plays a crucial role in the pathogenesis of UC when combined with cardiovascular disease. Both UC and AA share common inflammatory, environmental, and immune pathways, including dysregulation of cytokines such as Tumor Necrosis Factor-alpha (TNF-α), toll-like receptors, vascular endothelial growth factor, Interleukin-1 (IL-1), Interleukin-6 (IL-6), and lipopolysaccharides.

While the UC is a known risk factor for AA, the precise mechanisms linking the two diseases remain unclear. Inflammatory mediators are likely central to these overlapping pathways. In UC, T cells initiate the immune response and differentiate into Th1 and Th2 subtypes. T helper type 1 (Th1) cells secrete classical pro-

[1]Guizhou University of Traditional Chinese Medicine, Guiyang 550002, China. [2]The Second Affiliated Hospital of Guizhou University of Traditional Chinese Medicine, Guiyang 550002, China. [3]The First Affiliated Hospital of Guizhou University of Traditional Chinese Medicine, Guiyang 550001, China. ✉email: anzhenxiang057@gzy.edu.cn; 363110152@qq.com

inflammatory factors like interferon-gamma (IFN-γ), TNF-α, and Interleukin-2 (IL-2), which reduce gut mucus proteins and compromise the intestinal protective barrier[5]. TNF-α and IFN-γ contribute to atherosclerotic plaque growth. Meanwhile, T helper 17 (Th17) cells secrete Interleukin-17 (IL-17) and Interleukin-22 (IL-22), which increase reactive oxygen species, accelerating neointima formation and intraplaque bleeding. IL-17 can weaken the fibrous cap of atherosclerotic plaques, potentially leading to myocardial infarction[6]. Additionally, vascular smooth muscle cells in AA produce large amounts of extracellular matrix, secreting Monocyte Chemoattractant Protein-1 (MCP-1), Interleukin-1 beta (IL-1β), and IL-6. These molecules regulate neighboring cell function and release extracellular vesicles that promote vascular calcification[7].

Gene array technology allows researchers to measure gene expression data, enhancing the understanding of disease pathogenesis at the genetic level. Identifying common transcription factors (TFs) may offer novel insights into the shared pathogenesis of UC and AA. This study aimed to identify hub genes in UC associated with AA pathogenesis. These gene modules were then analyzed using Gene Ontology (GO), Kyoto Encyclopedia of Genes and Genomes (KEGG) pathway enrichment analysis, and Protein-Protein Interaction (PPI) network analysis to identify hub genes. Sixteen key hub genes were identified, their TFs were analyzed, and their expression was verified. These hub genes may provide valuable insights into the biological mechanisms underlying UC and AA.

Materials and methods

GEO data download and collation

Relevant gene expression datasets were retrieved from the GEO database using the keywords "UC" or "AA." The inclusion criteria were as follows: (1) The sequencing samples must be human; (2) The expression profiles for both diseases must be from the same sequencing platform (Affymetrix GPL570 platform, Affymetrix Human Genome U133 Plus 2.0 Array); (3) The gene expression profiles must include both case and control groups; (4) The dataset must provide processed data or raw data suitable for re-analysis. After screening, two datasets were downloaded: GSE28829, which includes 13 samples of early atherosclerotic (EA) and 16 samples of advanced atherosclerotic (AA) from human carotid arteries, and GSE36807, which includes 7 healthy control (HC) samples and 13 samples of UC.

Identification of DEGs

Differentially expressed genes (DEGs) for the analysis of UC and AA were extracted using the online analysis tool GEO2R (https://www.ncbi.nlm.nih.gov/geo/geo2r/)[8]. The screening criteria for DEGs were as follows: adjusted p-value < 0.05 and log2 fold change (FC) > 1. Gene differential expression was calculated using the "limma" package in R (R 4.2.2). The "ggplot2" package was used to plot gene heatmaps and volcano plots, with log2FC as the horizontal coordinate and -log10(P.adj) as the vertical coordinate. Additionally, the overlapping differentially expressed genes between UC and AA were visualized using the online Venn diagram tool (http://bioinformatics.psb.ugent.be/webtools/Venn/).

Functional enrichment analysis for DEGs

Differentially expressed genes that overlapped between UC and AA were analyzed for GO enrichment, which provides a simple annotation of the gene products in terms of biological pathways and cellular components involved in their function. KEGG[9] signaling pathway enrichment analysis was performed using the R package "clusterProfiler." A p-value of < 0.05 was used as the threshold for statistical significance.

PPI network analysis and hub gene identification

PPI network analysis was performed using the online database STRING (http://string-db.org)[10]. An interaction composite score > 0.4 was set as the threshold. PPI networks were visualized using Cytoscape software (http://www.cytoscape.org)[11]. TKey functional modules were analyzed using the Cytoscape plug-in MCODE, with the following settings: k-core = 2, degree cutoff = 2, max depth = 100, and node score cutoff = 0.2. Hub genes were identified using Cytoscape's cytoHubba plugin, with the Degree algorithm applied to determine the hub genes. A co-expression network for these hub genes was constructed using GeneMANIA[12].

Validation of hub genes expression with other data sets

Two datasets, GSE38713[13] and GSE100927[14], were used to validate the expression of mRNA for the identified hub genes. The two datasets validate the expression of mRNA for identified hub genes. The GSE38713 dataset consists of 13 healthy control colon samples, 8 inactive UC samples and 22 active UC samples. the GSE100927 dataset consists of 69 atherosclerotic samples and 35 control arterial samples. The two data sets were compared using a t-test, and a p-value < 0.05 suggested statistical significance.

Predicting TFs and validating

The Transcriptional Regulatory Relationships Unraveled by Sentence-based Text mining (TRRUST) is a manually annotated database of transcriptional regulatory networks[15], TRRUST contains the target genes corresponding to transcription factors and the regulatory relationships between transcription factors. patterns with 8,972 known regulatory messages, or 59.8%. Transcription factors regulating hub genes were obtained through the TRRUST database and finally the expression levels of transcription factors for hub genes were verified in GSE36807 and GSE28829 using a t-test and adjusted $p < 0.05$ was considered statistically significant.

Results

DEGs identification

The flowchart of our study is shown in Fig. 1. After standard processing of the dataset, the "limma" package in R software was used to visualize the volcano and heat maps of the DEGs in the two datasets. A total of 1,048 DEGs were identified in GSE36807 and 571 DEGs in GSE28829 (Fig. 2A,B). After performing an intersection of the Venn diagrams, 124 common DEGs were obtained. Upon removing genes with differing expression trends in GSE36807 and GSE28829, 13 downregulated DEGs and 92 upregulated DEGs were identified (Fig. 2C,D).

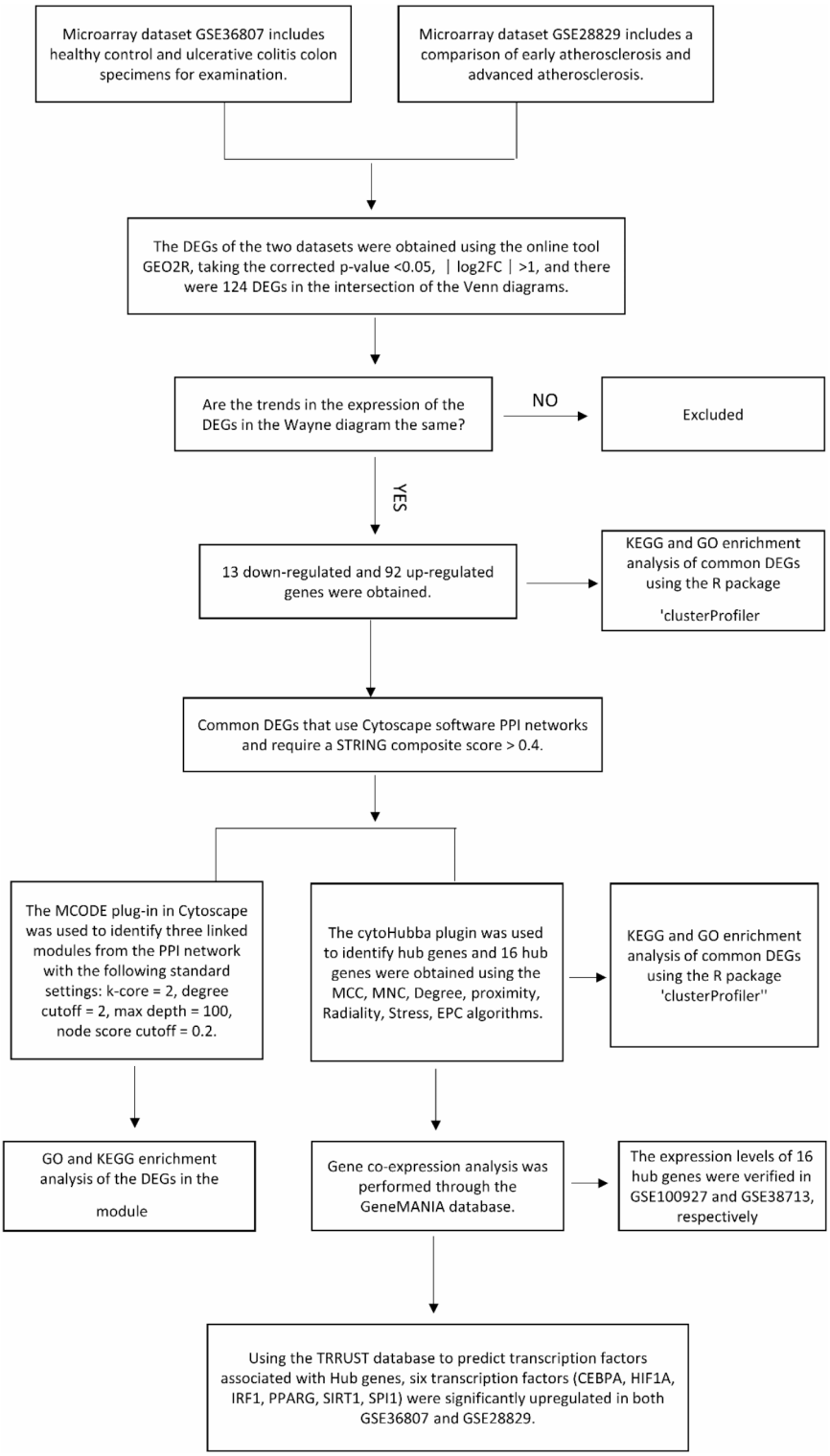

Fig. 1. Research design flow chart.

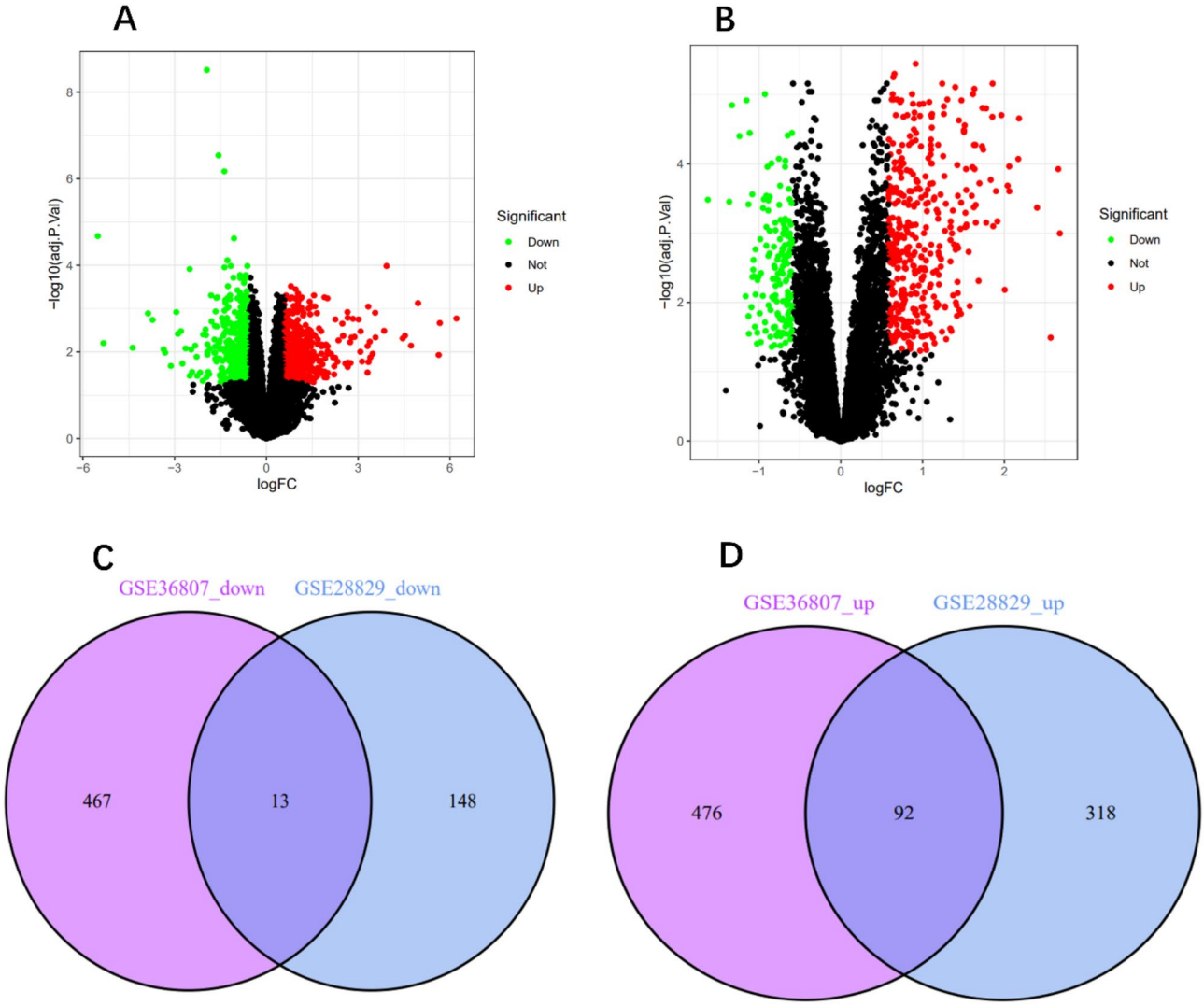

Fig. 2. UC and AA datasets. The volcano plot and Venn diagram of differentially expressed genes (DEGs). (**A**) Volcano plot of DEGs in GSE36807. (**B**) Volcano plot of DEGs in GSE28829; Upregulated genes are marked in light red; downregulated genes are marked in light green. (**C**) Venn diagrams of the GSE36807 and GSE28829 datasets showing down-regulation of DEGs. (**D**) Venn diagrams of the GSE36807 and GSE28829 datasets showing upregulated expression of DEGs.

Functional analysis of DEGs

To gain a more accurate understanding of the selected DEGs, the "clusterProfiler" package in R was used for enrichment analysis of GO and KEGG pathways. A filtering condition of adjusted $P < 0.05$ was applied, and the top 10 entries with the most significant GO and KEGG enrichments were selected. The results revealed that the DEGs were enriched in biological processes such as leukocyte migration, regulation of leukocyte migration, regulation of positive leukocyte migration, regulation of monocyte migration, regulation of extracellular infiltration, cytokine-mediated signaling pathways, and regulation of monocyte migration. In terms of cellular components, the DEGs were primarily associated with secretory granule membranes, tertiary granules, peptidase inhibitor complexes, paclitaxel-1-enriched granules, and specific granule membranes. They were also involved in protein complexes related to cell adhesion, specific granules, membrane rafts, and membrane microdomains.

Molecular functional analysis showed that the DEGs were significantly enriched in serine-type endopeptidase activity, serine-type peptidase activity, serine hydrolase activity, endopeptidase activity, integrin binding, extracellular matrix binding, pattern recognition receptor (PRR) activity, collagen binding, glycolipid binding, and G protein-coupled receptor binding (Fig. 3B). Important KEGG pathways enriched in the DEGs included Staphylococcus aureus infection, neutrophil extracellular trap formation, complement and coagulation cascades, lipid and arachidonic acid metabolism, leukocyte trans-endothelial migration, leishmaniasis, malaria, rheumatoid arthritis, the Nuclear Factor kappa-light-chain-enhancer of activated B cells (NF-κB) signaling pathway, and Coronavirus Disease 2019 (COVID-19) (Fig. 3C).

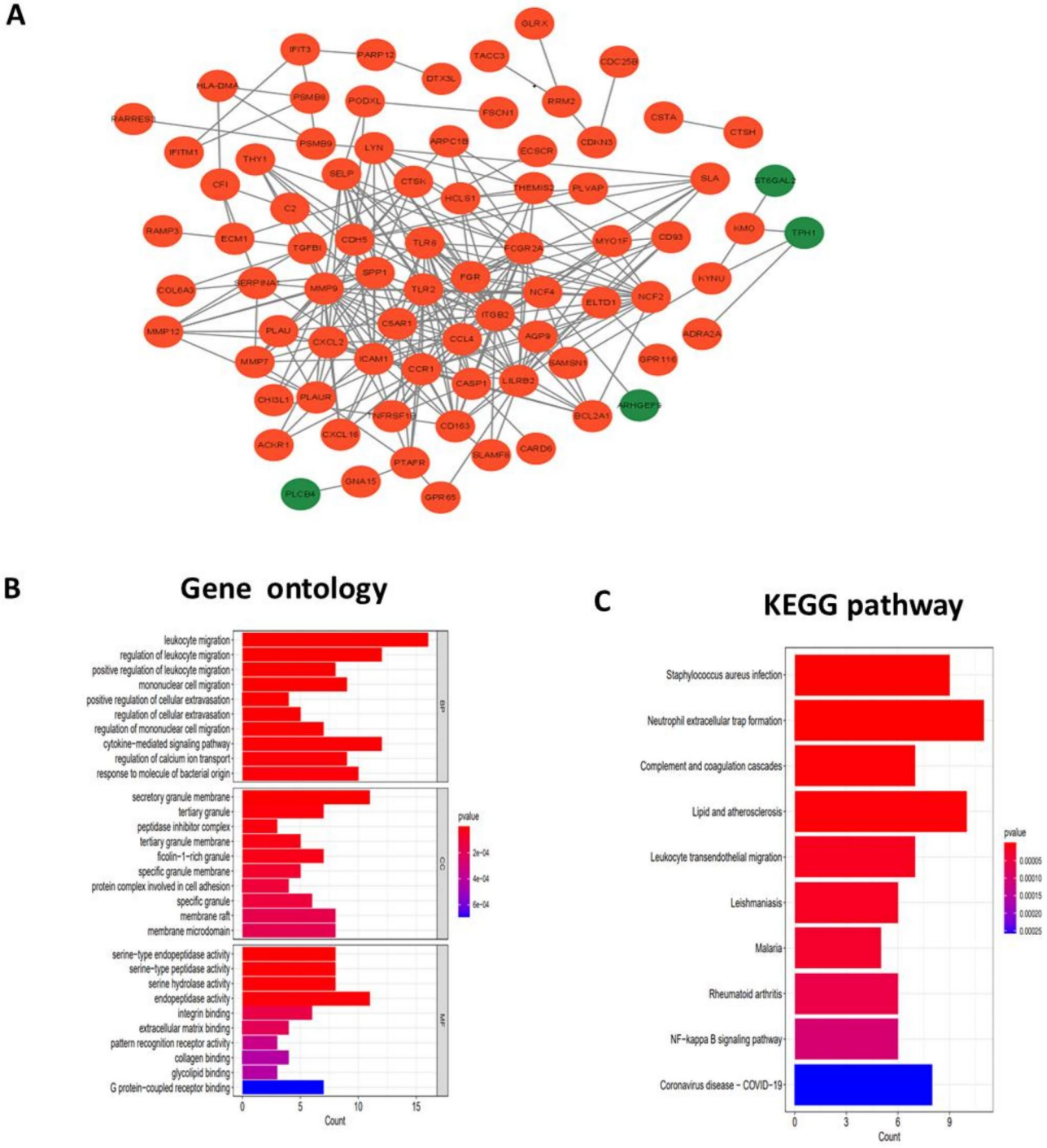

Fig. 3. Protein–protein interaction network and enrichment analysis of common DEGs. (**A**) PPI network diagram. Red indicates up-regulated genes, and green indicates down-regulated genes. (**B**,**C**) The enrichment analysis results of GO and KEGG Pathway. Adjusted P-value < 0.05 was considered significant.

Analysis of PPI networks

A PPI network of co-expressed genes with a composite score > 0.4 was constructed using Cytoscape, comprising 273 interaction pairs and 79 nodes (Fig. 3A). The MCODE plug-in in Cytoscape identified three closely related sub-network gene modules, which included 27 common differentially expressed genes and 73 interaction pairs (Fig. 4A–C). GO enrichment analysis of these genes revealed associations with inflammatory and immune responses, as well as NADPH responses (Fig. 4D). Additional pathways included migration, the Toll-like receptor (TLR) signaling pathway, and lipid and arachidonic acid metabolism (Fig. 4E).

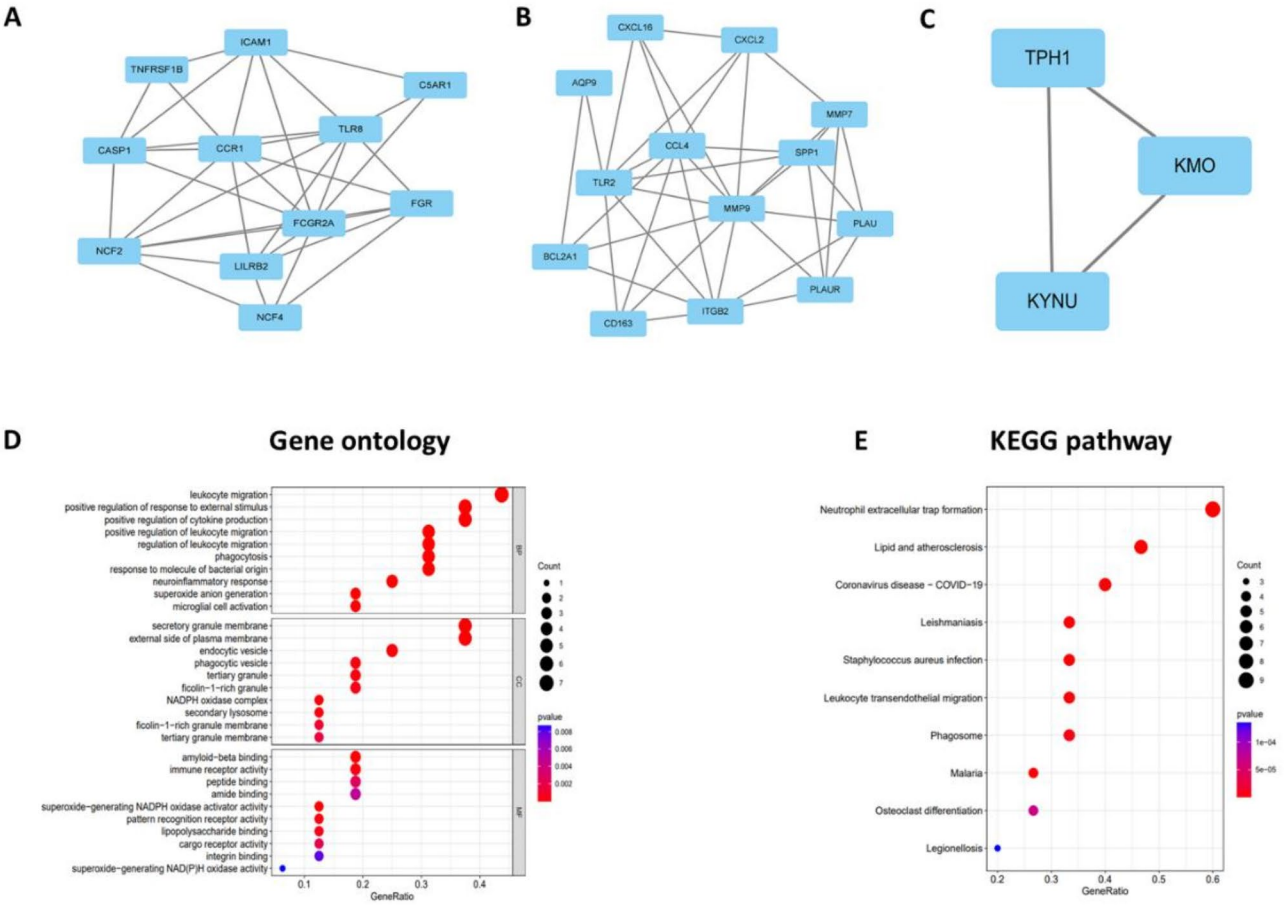

Fig. 4. GO and KEGG pathway enrichment analysis of differentially expressed genes in ulcerative colitis and atherosclerosis. (**A–C**) Are three closely related sub-network gene clustering modules. (**D**,**E**) is an enrichment analysis of the modular genes GO and KEGG. The size of their circles indicates the number of genes and the horizontal coordinates indicate the frequency of participating genes in the total genes. Statistical significance is represented by p-values, $p < 0.05$ indicating significant enrichment.

Selection and analysis of DEGs

The Cytoscape plugin cytoHubba was used to analyze the PPI network and identify hub genes. The top 16 hub genes (Table 1) were identified using the MCC, EPC, MNC, Degree, Closeness, and Radiality methods of the cytoHubba plugin (Fig. 5A). Their full names and associated functions are provided in Table 1. Based on the GeneMANIA database, the co-expression network and the functions associated with these genes were analyzed (Fig. 5B). GO analysis revealed that these genes are primarily involved in phagocytosis, superoxide anion production, leukocyte trafficking, neuroinflammatory responses, and superoxide metabolism processes (Fig. 5C), highlighting the crucial role of the inflammatory response in both disease processes. KEGG pathway analysis indicated that these genes are mainly involved in TLR signaling, phagosomes, neutrophil extracellular trap formation, lipid and arachidonic acid metabolism, and leukocyte migration across endothelial cells (ECs, Fig. 5D).

Validation and expression of DEGs

To assess the accuracy of the expression levels of these pivotal genes, this study selected two additional datasets: UC (GSE38713) and AA (GSE100927). The expression levels of the pivotal genes were analyzed, and the results showed that in UC (GSE38713), all pivotal genes except for the FGR gene were significantly upregulated in comparison to normal colon tissue (Fig. S1). In AA (GSE100927), the expression of all genes was higher in atherosclerotic plaques than in normal vascular tissue, except for TLR8, which had a missing expression value (Fig. S2).

Prediction and validation of TFs

A total of 16 TFs were predicted to regulate the expression of these genes, based on the TRRUST database (Fig. 6A; Table 2). Further validation revealed that six TFs (CEBPA, HIF1A, IRF1, PPARG, SIRT1, SPI1) were expressed at high levels in UC and AA (Fig. 6B, C). These TFs were found to synergistically regulate the hub genes CD163, ICAM1, TLR2, ITGB2, MMP9, and NCF2.

MCC	EPC	MNC	Degree	Closeness	Radiality
CCL4	ITGB2	ITGB2	ITGB2	ITGB2	ITGB2
TLR2	MMP9	MMP9	MMP9	MMP9	TLR2
ITGB2	CCL4	ICAM1	ICAM1	ICAM1	ICAM1
CCR1	ICAM1	TLR2	TLR2	TLR2	MMP9
TLR8	TLR2	CCL4	CCL4	CCL4	FCGR2A
FCGR2A	CCR1	CCR1	CCR1	CCR1	CCL4
NCF2	FCGR2A	NCF2	FCGR2A	FCGR2A	CCR1
LILRB2	NCF2	FCGR2A	LILRB2	NCF2	NCF2
FGR	TLR8	LILRB2	NCF2	LILRB2	LYN
ICAM1	FGR	FGR	FGR	FGR	FGR
CASP1	CASP1	TLR8	TLR8	TLR8	C5AR1
MMP9	LILRB2	CD163	CASP1	C5AR1	NCF4
CD163	SELP	CASP1	CD163	CD163	SELP
C5AR1	CD163	SELP	NCF4	NCF4	PLAUR
NCF4	NCF4	NCF4	SPP1	SELP	CD163
TNFRSF1B	C5AR1	SPP1	SELP	CASP1	LILRB2
SELP	BCL2A1	CXCL2	C5AR1	LYN	TLR8
CXCL2	TNFRSF1B	C5AR1	CXCL2	SPP1	CASP1
BCL2A1	CXCL2	CDH5	CDH5	CDH5	BCL2A1

Table 1. The top 16 hub genes rank in CytoHubba.

Discussion

Recent studies have increasingly confirmed the link between UC and AA. The pathogenesis of both UC and AA is related to chronic inflammation, primarily caused by abnormal endothelial cell function, oxidative stress, and an imbalance in cytokine secretion[16]. Research indicates that UC is influenced by genetic, immune, and environmental factors, leading to intestinal dysbiosis. This disruption allows the intestinal barrier to be compromised, enabling lipopolysaccharide (LPS) to cross the intestinal mucosal barrier, thereby activating immune and endothelial cells. This activation triggers inflammation and immune dysregulation, which contributes to the formation of atherosclerotic plaques[17]. In AA, Th1 cells are activated to produce pro-inflammatory cytokines such as IL-1, IL-6, and tumor necrosis factor (TNF), which in turn initiate a cascade of inflammatory responses. These cytokines further activate Th1 and Th17 cells, contributing to the development of UC. Both diseases are also linked to the activation of the Janus Kinase (JAK) and Signal Transducer and Activator of Transcription (STAT) pathways, which are downstream of cytokine-mediated lymphocyte activation, particularly with IL-6[18]. AA results from impaired metabolism of fatty substances deposited in the artery linings, including cholesterol, triglycerides, celiac particles, sphingolipids, ceramides, low-density lipoprotein (LDL), and apolipoproteins[19]. UC can be associated with AA through abnormal lipid metabolism, with studies showing a positive correlation between the degree of lipid abnormalities and the expression of inflammatory factors. Consequently, impaired lipid metabolism is positively associated with the severity of UC[20]. Furthermore, the intima-media thickness of the internal carotid artery is closely related to UC disease activity[21,22].

UC and AA may share similar pathogenic pathways, such as inflammatory and immunomodulatory pathways, which are intricately linked to the mechanisms underlying both diseases. The primary objective of this study was to identify common DEGs in UC and AA, in order to reveal potential therapeutic targets and predict the efficacy of biologic agents for treating UC complicated by AA. This study utilized bioinformatics analysis of two separate gene microarray datasets for UC and AA, sourced from the GEO database. A total of 105 common DEGs were identified in both diseases, including 16 hub genes (namely: CCL4, TLR2, ITGB2, CCR1, TLR8, FCGR2A, NCF2, LILRB2, FGR, ICAM1, CASP1, MMP9, CD163, C5AR1, NCF4, and SELP).

The results of GO enrichment analysis showed that these DEGs were mainly enriched in processes such as leukocyte migration, neuroinflammatory responses, and positive regulation of cytokine production. KEGG analysis revealed that the DEGs were primarily enriched in pathways associated with neutrophil extracellular trap formation, lipids and AA, Leishmaniosis, Staphylococcus aureus infection, leukocyte trans-endothelial migration, malaria, and COVID-19. These findings indicate that the identified genes are predominantly involved in inflammatory and immune pathways, where cytokines and chemokines play significant roles in the development and progression of UC and AA. For example, serum levels of IL-1β, IL-6, IL-17, and TNF-α are significantly elevated in both diseases and are key in their pathogenesis. In AA, TLR4 is a typical receptor in the innate immune response, activating the NF-κB signaling pathway and releasing AA-related inflammatory factors, such as IL-1β, IL-6, TNF-α, and IFN-γ[23]. In UC, antigen-presenting naïve T cells differentiate into T helper cell subtypes that produce cytokines. Elevated levels of IL-9 and IL-13 in the colonic mucosa led to abnormal barrier function, increased neutrophil migration, and heightened mucosal permeability[24]. Additionally, 16 TFs were identified that may regulate the expression of these genes.

Further validation revealed that six TFs were highly expressed in both UC and atherosclerotic plaques and were found to be synergistically involved in the regulation of six hub genes (namely: CD163, ICAM1,

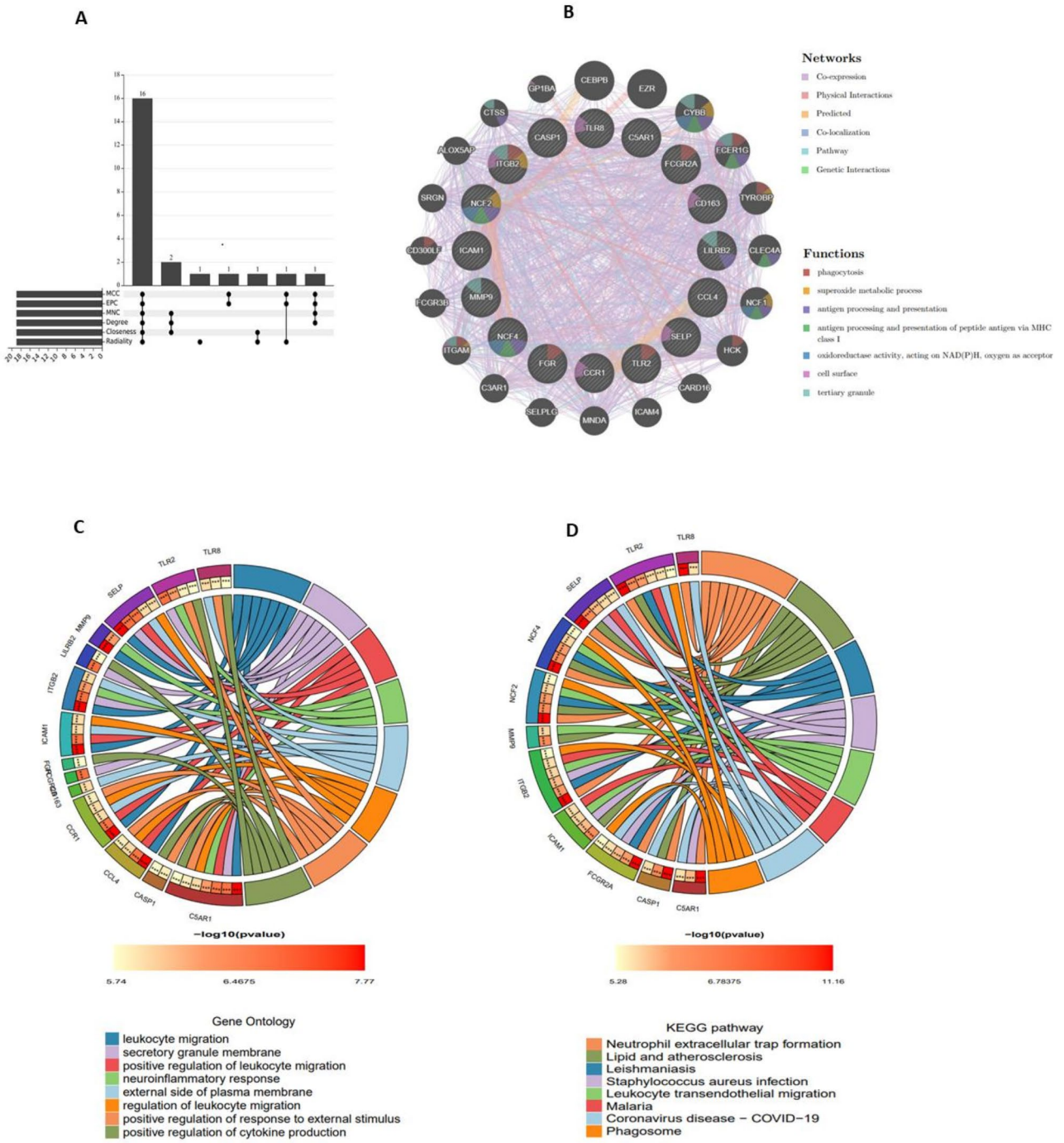

Fig. 5. Co-expression analysis and functional enrichment of hub genes identified in UC and AA. (**A**) Upset plot showing 16 overlapping hub genes screened by six algorithms. (**B**) Analysis of Hub genes and their co-expressed genes by GeneMANIA. (**C**,**D**) GO and KEGG enrichment analysis of the hub genes. The outermost circle is term on the right and the inner circle on the left represents the significant p-value of the corresponding pathway of the gene.

TLR2, ITGB2, MMP9, and NCF2). Among them, the CD163 is a protein primarily expressed on the surface of macrophages and serves as a marker of macrophage activation. CD163-expressing macrophages can upregulate the endothelial expression of Vascular Cell Adhesion Molecule (VCAM) on microvessels through the NF-κB signaling pathway, promoting the entry of inflammatory cells into the vessel wall, increasing vascular permeability, and accelerating atherosclerotic thrombosis[25]. Increased CD163 expression in UC has been linked to the presence of CD163 in macrophages derived from monocytes. Cross-linking of CD163 with EDHU1-Ab induces the secretion of pro-inflammatory cytokines, such as TNF-α, IL-1β, and IL-6, which contribute to enhanced mucosal inflammation[26]. Matrix metalloproteinase (MMP)-mediated protein hydrolysis plays a critical

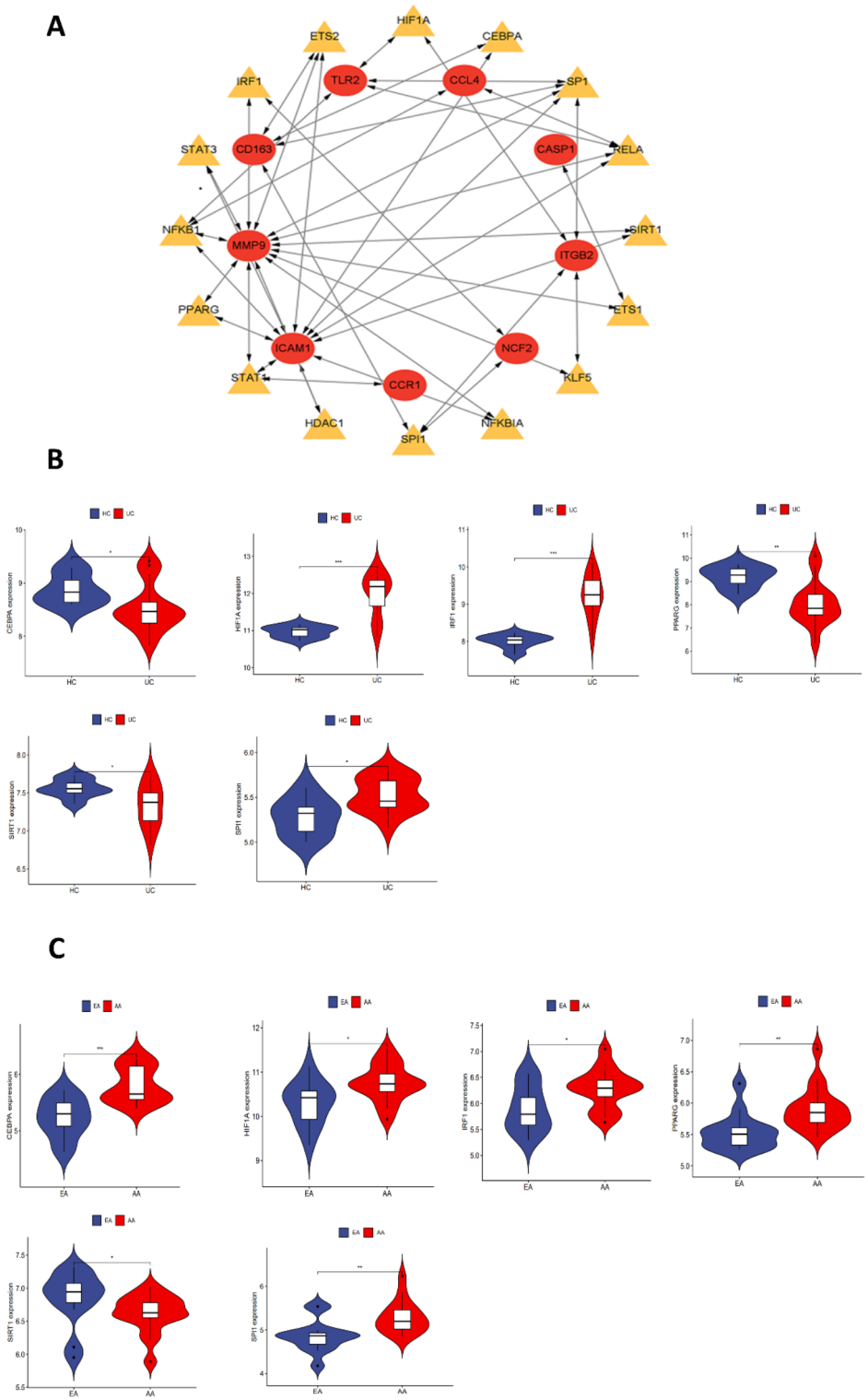

Fig. 6. TFs regulatory network and their expression in GSE36807 and GSE28829. (**A**) retrotransposon regulation, yellow represents retrotransposons, red represents hub genes. (**B**,**C**) expression levels of retrotransposons in GSE36807 and GSE28829. Comparison of the two data sets was performed using the mean t-test. p-value < 0.05 suggests statistical significance. *HC* health control, *UC* ulcerative colitis, *EA* early atherosclerotic, *AA* atherosclerotic. $^{*}p < 0.05$; $^{**}p < 0.01$; $^{****}p < 0.001$.

Key TF	Description	*p* value	List of overlapped genes
ETS2	v-ets erythroblastosis virus E26 oncogene homolog 2 (avian)	2.44E−06	CD163, MMP9, ICAM1
SPI1	Spleen focus forming virus (SFFV) proviral integration oncogene spi1	1.83E−05	NCF2, ITGB2, CD163
SP1	Sp1 transcription factor	3.33E−05	ITGB2, TLR2, ICAM1, MMP9, CD163
STAT1	Signal transducer and activator of transcription 1, 91 kDa	4.57E−05	MMP9, ICAM1, CCR1
KLF5	Kruppel-like factor 5 (intestinal)	5.23E−05	ITGB2, MMP9
RELA	v-rel reticuloendotheliosis viral oncogene homolog A (avian)	9.92E−05	CCL4, MMP9, ICAM1, TLR2
NFKB1	Nuclear factor of kappa light polypeptide gene enhancer in B-cells 1	0.000102	MMP9, ICAM1, CCL4, TLR2
NFKBIA	Nuclear factor of kappa light polypeptide gene enhancer in B-cells inhibitor, alpha	0.000114	ICAM1, MMP9
SIRT1	Sirtuin 1	0.000743	ICAM1, MMP9
CEBPA	CCAAT/enhancer binding protein (C/EBP), alpha	0.000839	ICAM1, CD163
IRF1	Interferon regulatory factor 1	0.000839	NCF2, MMP9
PPARG	Peroxisome proliferator-activated receptor gamma	0.0014	MMP9, ICAM1
HDAC1	Histone deacetylase 1	0.00162	MMP9, ICAM1
ETS1	v-ets erythroblastosis virus E26 oncogene homolog 1 (avian)	0.002	CASP1, MMP9
HIF1A	Hypoxia inducible factor 1, alpha subunit (basic helix-loop-helix transcription factor)	0.0022	TLR2, ITGB2
STAT3	Signal transducer and activator of transcription 3 (acute-phase response factor)	0.0063	MMP9, ICAM1

Table 2. Key transcriptional factors (TFs) of hub genes.

role in regulating cellular homeostasis and is involved in the signaling cascades of growth and inflammation. This occurs through the activation of cytokines and the release of sequestered growth factors. MMP9, a member of the MMP family, is an endoprotease with gelatinase activity that compromises endothelial integrity, disrupts collagen fiber production, and contributes to the thickening of the vessel wall, thus accelerating atherosclerotic thrombosis[27]. The generation and persistence of inflammation in UC are associated with MMP9 activity, which is induced by cytokines such as TNF-α and Transforming Growth Factor-beta (TGF-β). These cytokines enhance IL-8 and activate IL-1β, maintaining the pro-inflammatory process[28]. MMP9 also causes apoptosis of epithelial cells through proteolytic breakdown of the basement membrane, disrupting the epithelial barrier of the colonic mucosa and exacerbating the inflammatory response in the colon[29].

Intercellular Adhesion Molecule-1 (ICAM-1) is a transmembrane glycoprotein predominantly expressed in endothelial cells, epithelial cells, and immune cells. ICAM-1 binds to ITGB2 to regulate leukocyte adhesion and extravasation, controlling protein kinase C, proto-oncogene tyrosine protein kinase Src activity, and intracellular calcium signaling to regulate endothelial cell shape and vascular barrier function[30]. Studies have confirmed that in the gut epithelium, ICAM-1 expression levels are linked to neutrophil retention in the intestinal lumen, modulating intestinal permeability and delaying wound healing. Upregulation of ICAM-1 by pro-inflammatory cytokines in UC promotes leukocyte adhesion and extravasation into tissues, contributing to a prolonged inflammatory cycle in the colonic mucosa[30–32].

In AA, ECs can enhance NF-κB signaling, regulate the secretion of pro-inflammatory cytokines such as IL-1β and TNF-α, and induce ICAM-1 expression. This increases endothelial cell activation and enhances atherosclerotic plaque formation, directly contributing to the inflammatory response within the vessel wall[31,32]. TLR is a membrane PRR. TLR2 recognizes molecular patterns associated with various pathogens and plays a role in both the innate immune and inflammatory responses. TLR2 interacts with co-receptors to recruit bridging proteins such as Myeloid Differentiation Primary Response 88 (MyD88) or TRIF, which stimulate signaling pathways and induce the production of pro-inflammatory cytokines and chemokines[33]. Studies have shown that TLR2 regulates immune and epithelial cells in the gut, contributing to UC progression by increasing blood endotoxin levels and mediating inflammation[34]. TLR2 also promotes vascular smooth muscle cell migration to the intima during AA and contributes to coronary endothelial dysfunction following ischemia/reperfusion through the activation of neutrophils and free radical production. Therefore, TLR2 expression and activation can regulate the inflammatory process after vascular injury in a mouse model[35]. Integrin beta 2 (ITGB2), which encodes integrin β2, is an important regulator of cell survival, proliferation, adhesion, and migration[36]. ITGB2 promotes the trans-endothelial migration of leukocytes, disrupts endothelial barrier function, induces the release of pro-inflammatory factors, and participates in the inflammatory process in UC[37].

β2 integrins play a crucial role in adhesion during leukocyte recruitment, antigen presentation, pathogen clearance, and thrombosis, with their expression significantly increased in AA[38,39]. The NCF2 gene encodes neutrophil cytoplasmic factor 2 (p67phox), a component of NADPH oxidase, which plays an antibacterial, anti-inflammatory, and oxidative role in NADPH cellular functions. It is a major source of reactive oxygen species (ROS), which regulate cell proliferation, differentiation, and death[40]. Reduced NCF2 expression impairs NADPH oxidase complex synthesis and reduces ROS production, which may be involved in the pathogenesis of inflammatory autoimmune diseases and potentially in UC[41]. Oxidative stress is a key risk factor for AA, and NADPH is involved in AA inflammation through oxidative stress, triggering adverse effects such as thrombosis[42]. Currently, there are few direct studies investigating the involvement of NCF2 in UC and AA, highlighting the need for future research on this topic.

Several studies have demonstrated a significantly increased risk of atherosclerosis (AA) in patients with ulcerative colitis (UC). Measurements of carotid intima-media thickness (CIMT) have shown that UC

patients exhibit significantly higher CIMT values compared to healthy controls, indicating an elevated risk of early atherosclerosis. Furthermore, longer disease duration in UC patients is significantly associated with the progression of atherosclerosis[43]. The proportion of abnormal intima-media thickness in patients with active UC was significantly higher than in healthy controls (48.15% vs. 26.67%, $p = 0.05$), suggesting that active inflammation in UC may substantially increase the risk of subclinical atherosclerosis[44].

Metabolic abnormalities also play a critical role in AA development among UC patients. A study identified elevated homocysteine levels and insulin resistance as key predictors of atherosclerosis in UC patients[45]. Cardiovascular events are notably more frequent in older UC patients, particularly in those with additional cardiovascular risk factors, underscoring the need for targeted management in this population[46].

The critical role of inflammation in UC-associated AA has also been confirmed. Chronic inflammation in UC may directly lead to vascular endothelial injury and plaque formation through pro-inflammatory cytokines (e.g., TNF-α, IL-6) and their downstream signaling pathways (e.g., NF-κB)[47] Additionally, UC and AA share certain immune-regulatory pathways, such as Toll-like receptor signaling, suggesting potential common molecular mechanisms underlying these two conditions.

While previous studies have separately investigated key genes associated with UC[48] and AA[49], systematic exploration of their shared molecular mechanisms using bioinformatics approaches remains limited. This study integrated multiple independent datasets from the GEO database to identify common hub genes and associated transcription factors (TFs) between UC and AA and constructed complex interaction networks. Through these shared differentially expressed genes (DEGs), we successfully identified critical nodes, providing reliable preliminary evidence for elucidating the shared pathogenesis of UC and AA. The analytical results demonstrated high consistency across datasets and aligned with previously reported mechanisms, further validating the robustness of our findings.

However, this study has certain limitations. First, as the gene interaction networks were based on predictions from public databases, further experimental validation is required to elucidate the specific molecular mechanisms of the identified hub genes and TFs in UC and AA. Second, due to constraints in clinical sample availability and funding, we were unable to validate the expression levels of these key genes. Nonetheless, our findings underscore the significant risk of AA in UC patients, potentially driven by chronic inflammation, metabolic dysregulation, and immune regulatory abnormalities. Future studies should integrate clinical samples to further validate these molecular mechanisms and explore prevention and treatment strategies for AA in UC patients, thereby deepening our understanding of the pathological links between these two diseases.

Conclusions

This study investigated DEGs in UC and AA and explored their molecular processes using a bioinformatics method. In brief, the common DEGs for UC and AA were identified and enrichment and PPI network analyses were performed. A total of 16 hub genes (namely: CCL4, TLR2, ITGB2, CCR1, TLR8, FCGR2A, NCF2, LILRB2, FGR, ICAM1, CASP1, MMP9, CD163, C5AR1, NCF4, and SELP) and six TFc (namely: CEBPA, HIF1A, IRF1, PPARG, SIRT1, and SPI1) were jointly involved in the pathogenesis of both diseases. These mechanisms may be mediated by specific hub genes. The findings provide new insights into the molecular mechanisms of UC and AA, which can aid in the development of early diagnostic strategies, prognostic markers, and therapeutic targets.

Data availability

The datasets presented in this study can be found in online repositories. The names of the repository/repositories and accession number(s) can be found in the article. Further inquiries can be directed to the corresponding authors.

Received: 17 October 2024; Accepted: 19 March 2025
Published online: 28 March 2025

References

1. Bennett, M. R., Sinha, S. & Owens, G. K. Vascular smooth muscle cells in atherosclerosis. *Circ. Res.* **118**, 692–702. https://doi.org/10.1161/circresaha.115.306361 (2016).
2. Ungaro, R., Mehandru, S., Allen, P. B., Peyrin-Biroulet, L. & Colombel, J. F. Ulcerative colitis. *Lancet* **389**, 1756–1770. https://doi.org/10.1016/s0140-6736(16)32126-2 (2017).
3. Hudson, M. et al. Thrombotic vascular risk factors in inflammatory bowel disease. *Gut* **38**, 733–737. https://doi.org/10.1136/gut.38.5.733 (1996).
4. Panhwar, M. S. et al. Risk of myocardial infarction in inflammatory bowel disease: A population-based National study. *Inflamm. Bowel Dis.* **25**, 1080–1087. https://doi.org/10.1093/ibd/izy354 (2019).
5. Tatiya-Aphiradee, N., Chatuphonprasert, W. & Jarukamjorn, K. Immune response and inflammatory pathway of ulcerative colitis. *J. Basic Clin. Physiol. Pharmacol.* **30**, 1–10. https://doi.org/10.1515/jbcpp-2018-0036 (2018).
6. Taleb, S. & Tedgui, A. IL-17 in atherosclerosis: the good and the bad. *Cardiovasc. Res.* **114**, 7–9. https://doi.org/10.1093/cvr/cvx225 (2018).
7. Furmanik, M. et al. Endoplasmic reticulum stress mediates vascular smooth muscle cell calcification via increased release of Grp78 (glucose-regulated protein, 78 kDa)-loaded extracellular vesicles. *Arterioscler. Thromb. Vasc Biol.* **41**, 898–914. https://doi.org/10.1161/atvbaha.120.315506 (2021).
8. Barrett, T. et al. NCBI GEO: archive for functional genomics data sets—update. *Nucleic Acids Res.* **41**, D991–D995. https://doi.org/10.1093/nar/gks1193 (2013).
9. Kanehisa, M. & Goto, S. KEGG: Kyoto encyclopedia of genes and genomes. *Nucleic Acids Res.* **28**, 27–30 (2000).
10. Franceschini, A. et al. STRING v9.1: protein-protein interaction networks, with increased coverage and integration. *Nucleic Acids Res.* **41**, D808–D815. https://doi.org/10.1093/nar/gks1094 (2013).
11. Smoot, M. E., Ono, K., Ruscheinski, J., Wang, P. L. & Ideker, T. Cytoscape 2.8: new features for data integration and network visualization. *Bioinformatics* **27**, 431–432. https://doi.org/10.1093/bioinformatics/btq675 (2011).

12. Warde-Farley, D. et al. The genemania prediction server: biological network integration for gene prioritization and predicting gene function. *Nucleic Acids Res.* **38**, W214–W220. https://doi.org/10.1093/nar/gkq537 (2010).
13. Planell, N. et al. Transcriptional analysis of the intestinal mucosa of patients with ulcerative colitis in remission reveals lasting epithelial cell alterations. *Gut* **62**, 967–976. https://doi.org/10.1136/gutjnl-2012-303333 (2013).
14. Steenman, M. et al. Identification of genomic differences among peripheral arterial beds in atherosclerotic and healthy arteries. *Sci. Rep.* **8**, 3940. https://doi.org/10.1038/s41598-018-22292-y (2018).
15. Han, H. et al. TRRUST v2: an expanded reference database of human and mouse transcriptional regulatory interactions. *Nucleic Acids Res.* **46**, D380–D386. https://doi.org/10.1093/nar/gkx1013 (2018).
16. Nuñez, P., García Mateo, S., Quera, R. & Gomollón, F. Inflammatory bowel disease and the risk of cardiovascular diseases. *Gastroenterol. Hepatol.* **44**, 236–242. https://doi.org/10.1016/j.gastrohep.2020.09.002 (2021).
17. Bigeh, A., Sanchez, A., Maestas, C. & Gulati, M. Inflammatory bowel disease and the risk for cardiovascular disease: does all inflammation lead to heart disease? *Trends Cardiovasc. Med.* **30**, 463–469. https://doi.org/10.1016/j.tcm.2019.10.001 (2020).
18. Weissman, S. et al. Atherosclerotic cardiovascular disease in inflammatory bowel disease: the role of chronic inflammation. *World J. Gastrointest. Pathophysiol.* **11**, 104–113. https://doi.org/10.4291/wjgp.v11.i5.104 (2020).
19. Malekmohammad, K., Bezsonov, E. E. & Rafieian-Kopaei, M. Role of lipid accumulation and inflammation in atherosclerosis: focus on molecular and cellular mechanisms. *Front. Cardiovasc. Med.* **8**, 707529. https://doi.org/10.3389/fcvm.2021.707529 (2021).
20. Liu, Z. et al. Dyslipidaemia is associated with severe disease activity and poor prognosis in ulcerative colitis: A retrospective cohort study in China. *Nutrients* **14**, 40. https://doi.org/10.3390/nu14153040 (2022).
21. Goshayeshi, L. et al. Association between carotid intima-media thickness and ulcerative colitis: a systematic review and meta-analysis. *Electron. Phys.* **10**, 6956–6964. https://doi.org/10.19082/6956 (2018).
22. Ekmen, N. et al. Evaluation of epicardial adipose tissue and carotid intima-media thickness as a marker of atherosclerosis in patients with inflammatory bowel disease. *Rev. Esp. Enferm Dig.* **113**, 643–648. https://doi.org/10.17235/reed.2020.7394/2020 (2021).
23. Zhu, Y. et al. Research progress on the relationship between atherosclerosis and inflammation. *Biomolecules* **8**, 80. https://doi.org/10.3390/biom8030080 (2018).
24. Nakase, H., Sato, N., Mizuno, N. & Ikawa, Y. The influence of cytokines on the complex pathology of ulcerative colitis. *Autoimmun. Rev.* **21**, 103017. https://doi.org/10.1016/j.autrev.2021.103017 (2022).
25. Guo, L. et al. CD163 + macrophages promote angiogenesis and vascular permeability accompanied by inflammation in atherosclerosis. *J. Clin. Investig.* **128**, 1106–1124. https://doi.org/10.1172/jci93025 (2018).
26. Franzè, E. et al. Lesional accumulation of CD163-expressing cells in the gut of patients with inflammatory bowel disease. *PLoS ONE* **8**, e69839. https://doi.org/10.1371/journal.pone.0069839 (2013).
27. Cowan, K. N., Jones, P. L. & Rabinovitch, M. Elastase and matrix metalloproteinase inhibitors induce regression, and tenascin-C antisense prevents progression, of vascular disease. *J. Clin. Investig.* **105**, 21–34. https://doi.org/10.1172/jci6539 (2000).
28. Marshall, D. C. et al. Selective allosteric Inhibition of MMP9 is efficacious in preclinical models of ulcerative colitis and colorectal cancer. *PLoS ONE* **10**, e0127063. https://doi.org/10.1371/journal.pone.0127063 (2015).
29. Grossmann, J. Molecular mechanisms of detachment-induced apoptosis–Anoikis. *Apoptosis* **7**, 247–260. https://doi.org/10.1023/a:1015312119693 (2002).
30. Wiesolek, H. L. et al. Intercellular adhesion molecule 1 functions as an efferocytosis receptor in inflammatory macrophages. *Am. J. Pathol.* **190**, 874–885. https://doi.org/10.1016/j.ajpath.2019.12.006 (2020).
31. Cao, X., Wu, Y., Hong, H. & Tian, X. Y. Sirtuin 3 dependent and independent effects of NAD(+) to suppress vascular inflammation and improve endothelial function in mice. *Antioxidants (Basel)* **11**, 706. https://doi.org/10.3390/antiox11040706 (2022).
32. Ding, S. et al. ICAM-1-related noncoding RNA accelerates atherosclerosis by amplifying NF-κB signaling. *J. Mol. Cell. Cardiol.* **170**, 75–86. https://doi.org/10.1016/j.yjmcc.2022.06.001 (2022).
33. Shmuel-Galia, L. et al. Neutralization of pro-inflammatory monocytes by targeting TLR2 dimerization ameliorates colitis. *EMBO J.* **35**, 685–698. https://doi.org/10.15252/embj.201592649 (2016).
34. Yang, C. et al. Relationship between small intestinal bacterial overgrowth and peripheral blood ET, TLR2 and TLR4 in ulcerative colitis. *J. Coll. Phys. Surg. Pak.* **30**, 245–249. https://doi.org/10.29271/jcpsp.2020.03.245 (2020).
35. Roshan, M. H., Tambo, A. & Pace, N. P. The role of TLR2, TLR4, and TLR9 in the pathogenesis of atherosclerosis. *Int. J. Inflamm.* **2016**, 1532832. https://doi.org/10.1155/2016/1532832 (2016).
36. Zhang, Y. & Wang, H. Integrin signalling and function in immune cells. *Immunology* **135**, 268–275. https://doi.org/10.1111/j.1365-2567.2011.03549.x (2012).
37. Dunne, J. L., Collins, R. G., Beaudet, A. L., Ballantyne, C. M. & Ley, K. Mac-1, but not LFA-1, uses intercellular adhesion molecule-1 to mediate slow leukocyte rolling in TNF-alpha-induced inflammation. *J. Immunol.* **171**, 6105–6111. https://doi.org/10.4049/jimmunol.171.11.6105 (2003).
38. Rosetti, F. & Mayadas, T. N. The many faces of Mac-1 in autoimmune disease. *Immunol. Rev.* **269**, 175–193. https://doi.org/10.1111/imr.12373 (2016).
39. Lv, X. et al. Differential gene expression and immune cell infiltration in carotid intraplaque hemorrhage identified using integrated bioinformatics analysis. *Front. Cardiovasc. Med.* **9**, 818585. https://doi.org/10.3389/fcvm.2022.818585 (2022).
40. Breitenbach, M. et al. The defense and signaling role of NADPH oxidases in eukaryotic cells: review. *Wien Med. Wochenschr.* **168**, 286–299. https://doi.org/10.1007/s10354-018-0640-4 (2018).
41. Zhou, Y. et al. Evidence for a direct link between PAD4-mediated citrullination and the oxidative burst in human neutrophils. *Sci. Rep.* **8**, 15228. https://doi.org/10.1038/s41598-018-33385-z (2018).
42. Marqués, J., Cortés, A., Pejenaute, Á. & Zalba, G. Implications of NADPH oxidase 5 in vascular diseases. *Int. J. Biochem. Cell. Biol.* **128**, 105851. https://doi.org/10.1016/j.biocel.2020.105851 (2020).
43. Popa, I. V. et al. P232 atherosclerosis in ulcerative colitis. *J. Crohn's Colitis* **11**, S195–S196 (2017).
44. Lasa, J. et al. Endoscopically active ulcerative colitis is associated with asymptomatic atherosclerotic vascular disease: A case-control study. *Inflamm. Bowel Dis.* **30**, 1654–1661. https://doi.org/10.1093/ibd/izad217 (2024).
45. Jain, S. S. et al. Early atherosclerosis in ulcerative colitis: cross-sectional case-control study. *J. Dig. Dis.* **16**, 656–664. https://doi.org/10.1111/1751-2980.12297 (2015).
46. Patel, S. M., Venkatesan, V., Sigman, K. M. & Dugum, M. F. Type Vb double common bile duct: A rare case associated with cholangiocarcinoma. *Cureus* **16**, e70118. https://doi.org/10.7759/cureus.70118 (2024).
47. Negreanu, A. M., Stemate, A., Spataru, T. & Negreanu, L. J. *Early Atherosclerosis and Acute Vascular Events in Ulcerative Colitis Patients—A Case Series* (2022).
48. Zhang, J. et al. Investigation of potential genetic biomarkers and molecular mechanism of ulcerative colitis utilizing bioinformatics analysis. *Biomed. Res. Int.* **2020**, 4921387. https://doi.org/10.1155/2020/4921387 (2020).
49. Lawrence, M. G. et al. Patient-derived models of abiraterone- and enzalutamide-resistant prostate cancer reveal sensitivity to ribosome-directed therapy. *Eur. Urol.* **74**, 562–572. https://doi.org/10.1016/j.eururo.2018.06.020 (2018).

Author contributions

M.W., D. L. conceived the research design and analyzed the data. X. X., Q. S., Y. X., and L.S. wrote the manuscript. Z. A. and X. Y. provide supervision and funding. All authors reviewed the manuscript and agreed to publish it.

Funding
This work was supported by the National Natural Science Foundation of China (No.82360978); the Fifth National Training Program for Excellent Clinical Talents in Traditional Chinese Medicine of the State Administration of Traditional Chinese Medicine (No. Guozhong Medicine Renjiao [2022] No.1); Guizhou University of Traditional Chinese Medicine Chinese Medicine Spleen and Stomach Disease Science and Technology Innovation Talent Team Construction (No. Guizhou Chinese Medicine TD [2022] No.005).

Declarations

Competing interests
The authors declare no competing interests.

Consent for publication
We confirm that this work is original and has not been published elsewhere, nor is it currently under consideration for publication elsewhere. And all authors have approved the manuscript for submission.

Additional information
Supplementary Information The online version contains supplementary material available at https://doi.org/10.1038/s41598-025-95125-4.

Correspondence and requests for materials should be addressed to Z.A. or X.Y.

Reprints and permissions information is available at www.nature.com/reprints.

Publisher's note Springer Nature remains neutral with regard to jurisdictional claims in published maps and institutional affiliations.